Nonlinear stability of solitons against strong external perturbations

F. B. Rizzato,[1,2] G. I. de Oliveira,[3] and A. C.-L. Chian[2,4]
[1]*Instituto de Física, Universidade Federal do Rio Grande do Sul, Caixa Postal 15051, 91501-970 Porto Alegre, Rio Grande do Sul, Brazil*
[2]*World Institute for Space Environment Research–WISER, NITP, Adelaide University, Adelaide, South Australia 5005, Australia*
[3]*Departamento de Biociências, Campus de Aquidauana, Universidade Federal do Mato Grosso do Sul, Caixa Postal 135, 79200-000, Aquidauana, Mato Grosso do Sul, Brazil*
[4]*National Institute for Space Research–INPE, P.O. Box 515, 12227-010 São José dos Campos, São Paulo, Brazil*
(Received 6 September 2002; revised manuscript received 24 January 2003; published 28 April 2003)

We study soliton stability under the action of strong external perturbations. Limits on the weak perturbation approach are established with the help of average Lagrangian methods and full simulations. We found that for the same relative perturbation, larger amplitude solitons develop instability earlier than weaker amplitude solitons.

DOI: 10.1103/PhysRevE.67.047601 PACS number(s): 05.45.Yv

We investigate solitary wave stability under the action of strong time-dependent perturbations. Our localized waves are loosely called ''solitons'' even though this is a terminology reserved for integrable sets, which is not the case here. Schrödinger solitons generated by the nonlinear Schrödinger equation (NLSE for short) are the focus of our study. They are of relevance in modeling slow modulations of high-frequency fields, such as in solid state waves, lasers, hydrodynamic waves, Langmuir turbulence in plasma physics, electromagnetic radiation in pulsars, and others [1–5]. If solitons are perturbed they can emit radiation, as is the case of Schrödinger solitons perturbed by density waves in Langmuir turbulence. Solitons can actually emit a variety of waves, but one of the most persistent types results from the conversion of trapped *quanta* within the soliton into free modes. Since in this case the radiated field is of the same nature as the field forming the soliton, the problem is better analyzed with help of a perturbed NLSE. More complex kinds of radiation occur in shorter time scales and do not interfere with the present process [6,7]. Weak instability has been the subject of attention of a large number of works [1,8] and the conclusions point to the fact that when solitons are weakly perturbed, they turn into quiescent sources emitting low-amplitude radiation. Calculations in this weak regime take into account the slowness of the process. One supposes that the unperturbed problem is solvable by inverse scattering techniques, a soliton is given as a steady entity, and emitted radiation is obtained perturbatively. In a final step, one makes use of a quasilinear approximation to evaluate radiative reaction and obtain slowly varying solitonic characteristics. Given the soliton amplitude η and, generically, the amplitude of the perturbing terms A, the technique has been argued to be effective if the smallness condition $A \ll \eta^2$ holds. Our interest here is to examine how far can one trust this smallness condition and what happens beyond. Failure of the method occurs if the process is so fast that the soliton cannot be seen as a quasistatic entity. Then, alternative procedures are required to make proper estimates. What we propose in this paper is to make use of average Lagrangian techniques [7,8] to determine the accuracy of the quiescent approach. Our procedure is quite direct. We model the soliton and the accompanying perturbing terms with a finite number of degrees of freedom (DOFs)—the so called collective DOFs—and determine appropriate dynamical equations for these DOFs based on averages of the governing Lagrangian. The method is not afflicted by any constraints on the size of the perturbing terms. We will see that strong instabilities with appreciable radiation emission result from resonant interactions involving oscillation of the DOFs associated with the soliton solution and oscillations of the time-dependent external drive. Alternative approaches overlooking the internal solitonic oscillations does not reveal regions of strong instabilities [9], so we may consider the Lagragian averages as of considerable help here. Schrödinger solitons are obtained from the perturbed NLSE which in turn approximates the Zakharov equations [10]:

$$iE_t + E_{xx} + 2nE = 0, \quad n_{tt} - n_{xx} = -(|E|^2)_{xx}. \tag{1}$$

The Zakharov set (1) generically describes the nonlinear interaction of the amplitude $E(x,t)$ of a high-frequency field with a full low-frequency field $n(x,t)$. We split $n(x,t)$ in the form $n(x,t) = n_{nh}(x,t) + n_h(x,t)$ with $n_h(x,t)$ as the homogeneous solution of the second Eq. (1) and $n_{nh}(x,t)$ as some functional form of $|E(x,t)|^2$ [3] that may be extended to include a variety of additional nonlinear features such as electronic mass correction due to relativistic effects and higher-harmonic density oscillations as discussed in the context of pulsar radiation [4,5]. In several cases of interest the standing wave $n_h(x,t) = A\cos(kx)\cos(\omega t)$ is representative. $\omega = \omega(k) = k$ is the dispersion relation and A is the amplitude of the perturbation colliding with the solitary structure. n_h could represent the action of an isotropic distribution of ion-acoustic waves on electromagnetic solitons, for instance. The interest here would be on how robust is the solitary wave. Since solitons are characterized by a few DOFs, their destruction would be connected with the appearance of high-dimensional spatiotemporal chaos. Alternatively, one could argue that while solitons are present the quiescent approach is validated. Solitary solutions of the Zakharov equations (1) have their own characteristic or breathing frequencies, ω_e and ω_n, which are, respectively, associated with shape fluctuations of the E and n fields [2,7,8,11]. $\omega_e \sim O(|E|^2)$ and $\omega_n \sim O(|E|)$ [7], so when the fields are sufficiently small that $|E|^2 \ll 1$, $\omega_e \ll \omega_n$ as well. In this so-called subsonic case $n_{nh}(x,t) = |E(x,t)|^2$, but recent results show that even when $|E|^2 \sim 1$ the previous expression for n_{nh} as a function of E is approximately valid [7,12]. So the final system we will be integrating is

$$iE_t + E_{xx} + 2|E|^2 E = -2A\cos(kx)\cos(\omega t)E, \tag{2}$$

for $|E|^2 \ll 1$ up to $|E|^2 \sim 1$. If $A=0$ in Eq. (2), one finds a stationary solitary solution in the form $E = E_s(x,t) = \eta_0 \operatorname{sech}(\eta_0 x) e^{i\eta_0^2 t}$ with η_0 as an arbitrary positive amplitude parameter. When the perturbation is present but sufficiently small with $A \ll 1$, the soliton can be seen as a quasistatic structure. Its slowly time-varying amplitude $\eta = \eta(t)$ is then controlled by an expression obtained via inverse scattering methods, considering oppositely propagating perturbing waves with equal amplitudes,

$$\dot{\eta} = -\frac{1}{8}\frac{(\pi A k)^2}{\sqrt{k-\eta^2}}\left[\operatorname{sech}^2\left(\frac{\pi}{2\eta}(\sqrt{k-\eta^2}+k)\right) + \operatorname{sech}^2\left(\frac{\pi}{2\eta}(\sqrt{k-\eta^2}-k)\right) + 2\operatorname{sech}\left(\frac{\pi}{2\eta}(\sqrt{k-\eta^2}+k)\right)\operatorname{sech}\left(\frac{\pi}{2\eta}(\sqrt{k-\eta^2}-k)\right)\right], \tag{3}$$

$\eta(t=0) = \eta_0$ [1]. Note that only solitons with vanishing velocities are considered. They are favored in Langmuir turbulence [13] and this is consistent with the fact that the perturbing wave can be decomposed into right- and left-ward propagating modes with equal amplitudes. If this symmetry were violated, solitons would acquire nonzero velocities that should appear in quiescent formulas like Eq. (3) [9]. Another point to be observed from Eq. (3) is that under quiescent conditions, radiation is present only when $k > \eta^2$. Within the range $0 < k < \eta^2$ solitons can even vibrate, but do not radiate. Let us now proceed to the numerical work. All simulations are based on a pseudospectral decomposition associated with a Bulirsch-Stöer method. Solitary waves are placed at the center of the simulation box with peak at $x=0$ and with E_s at $t=0$ as the initial condition. The length L of the system is much larger than that of solitons, $L = 60 \times (1/\eta_0)$, and the temporal variable $\tau \equiv \omega t/2\pi$ used in the figures measures the number of cycles of the perturbing drive n_h; $j \equiv Nx/L$ is a scaled distance. Small dissipation is added for $|x| > (3/4)(L/2)$ to emulate open boundaries; i.e., radiation does not return to the soliton once it is emitted. Then, we first consider two contrasting situations for a small value $A = 0.01\,\eta_0^2$ and a relatively small $\eta_0 = 0.2$: $k = 0.5\,\eta_0^2$ and $k = 2.5\,\eta_0^2$. Both cases are discussed in the context of Fig. 1. In panels (a) and (b) of Fig. 1, we plot contours of $|E(x,t)|$ to perform a preparatory comparative study on soliton positioning as function of time; $k = 2.5\eta_0^2$. In panel (a), we briefly relax our standing wave assumptions and consider a rightward moving perturbing wave $n_h = A\cos(kx - \omega t)$ and in panel (b) we return to our standing perturbations n_h

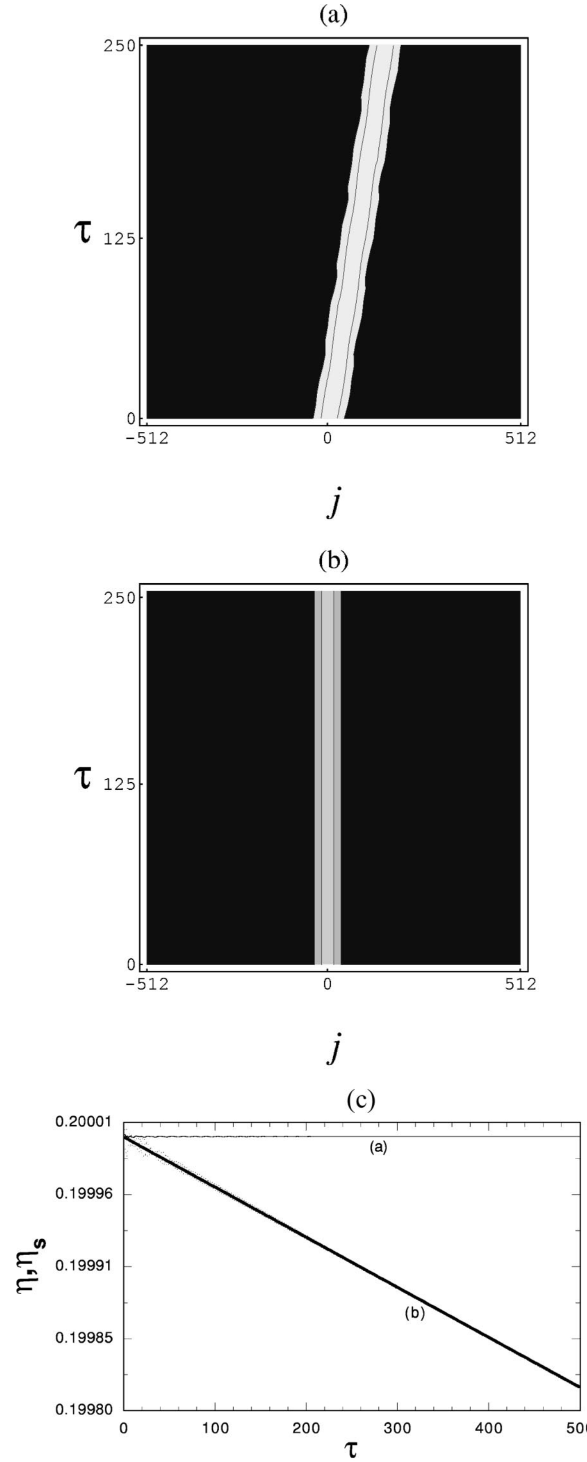

FIG. 1. Panels (a) and (b) contour plots of $|E(x,t)|$ for $k = 2.5\eta_0^2$; lighter shades $\Rightarrow$ higher intensities. Panel (c) $\eta_s \equiv |E(x=0,t)|$ vs τ; $k = 0.5\eta_0^2$ in curve (a), and $k = 2.5\eta_0^2$ in curves (b), where dots represent simulations. In all panels, $\eta_0 = 0.2$, $A/\eta_0^2 = 0.01$, and $\tau \equiv \omega t/2\pi$.

$= A\cos(kx)\cos(\omega t)$. In agreement with our earlier comments, the soliton is stationary only in case (b). In case (a) nonzero velocities develop and should be taken into account in quiescent formulas. In Fig. 1(c), we investigate the time evolution of variable $\eta_s \equiv |E(x=0,t)|$ in the standing wave situa-

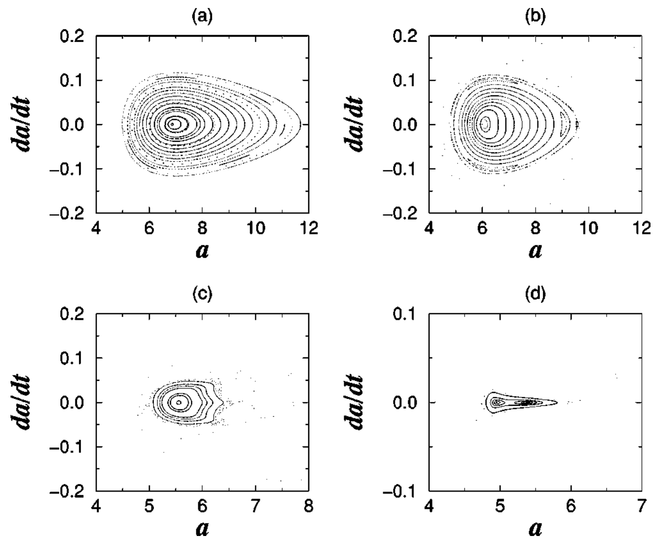

FIG. 2. Poincaré plots for $\eta_0=0.2$ and $k=0.5\eta_0^2$. $\varepsilon=0.1$ in (a), $\varepsilon=1.0$ in (b), $\varepsilon=2.0$ in (c), and $\varepsilon=2.4$ in (d).

tion. A series of curves are drawn. Curve (a), where $k=0.5\eta_0^2$, represents the results of full simulations, and curves (b), where $k=2.5\eta_0^2$, display the results of a full run recorded as dots, superposed with the results of numerical integration of Eq. (3) shown as a thick solid line. The solid line is closely surrounded by dots, so it is indeed seen that agreement for such a small A is excellent when $k>\eta_0^2$, and that when $k<\eta_0^2$ no decay is observable as predicted by the quiescent approach. One goes further since the issue here is to determine up to what extent arbitrarily perturbed solitons are still quasistructures of the system. We focus on the subsystem composed by solitons and the external drive. Perhaps the best way to analyze soliton stability under the action of strong perturbing fields is the average Lagrangian method. One first considers the full Lagrangian for the E field from which the exact equation (2) is to be obtained through Euler-Lagrange equations

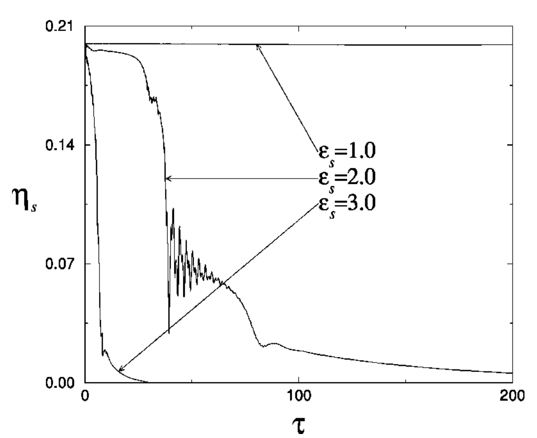

FIG. 3. η_s vs τ for $\eta_0=0.2$, $k=0.5\eta_0^2$, and various values of ε_s.

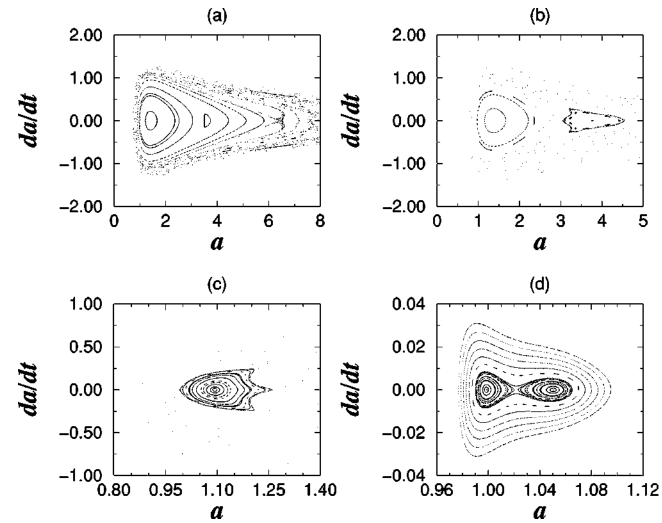

FIG. 4. Poincaré plots for $\eta_0=1.0$ and $k=0.5\eta_0^2$. $\varepsilon=0.001$ in (a), $\varepsilon=0.01$ in (b), $\varepsilon=0.1$ in (c), and $\varepsilon=0.14$ in (d).

$$L=\int_{-\infty}^{+\infty}\mathcal{L}dx,$$

$$\mathcal{L}\equiv\frac{i}{2}(E^*E_t-EE_t^*)-|E_x|^2+|E|^4+2n_h(x,t)|E|^2, \quad (4)$$

$i^2=-1$. Then one supposes an ansatz solitonic form for E with a few time-dependent parameters and known spatial dependence. The ansatz is inserted into Eq. (4), spatial integrations are performed, and the dynamics of the time-dependent parameters is obtained. If this reduced dynamics is stable against the action of n_h solitons might be indeed quasistructures of the full system. Otherwise, one can expect the absence of solitons and the breakdown of the quiescent approach. The following ansatz has been shown to be useful $E=E_a(x,t)=\sqrt{W/a(t)}\exp[-x^2/2a(t)^2+i\phi(t)+ik(t)x^2]$, since it resembles the solitary solution E_s and is analytically treatable in view of the fact that the spatial dependence appears only in exponential functions [1,2]. $a(t)$ is the soliton width, W is a constant measuring the number of quanta involved in the dynamics, and $k(t)$ is the chirp factor. W is obtained via $W=(1/\sqrt{\pi})\int_{-\infty}^{+\infty}|E_a(x,t)|^2dx$ and shall be similarly related to the quanta of the full static solution E_s: $W=(1/\sqrt{\pi})\int_{-\infty}^{+\infty}|E_s(x,t)|^2dx=2\eta_0/\sqrt{\pi}$. In other words, if one defines a static solution E_s via η_0, W corresponding to the ansatz is promptly determined. Then if one calculates the average Lagrangian from Eq. (4) and applies Euler-Lagrange prescriptions to variables a,ϕ,k, the governing equations for the width variable $a=a(t)$ is obtained

$$\ddot{a}(t)=\frac{4}{a(t)^3}-\frac{2\sqrt{2}W}{a(t)^2}-4Ak^2a(t)\cos(kt)e^{-(k^2a(t)^2/4)}. \quad (5)$$

$a=\sqrt{2}/W$ is the stable equilibrium in the absence of perturbation. We launch a number of orbits around this unperturbed equilibrium, with $A\neq 0$, and analyze the corresponding surface of section $(a(t),\dot{a}(t))$ at $kt=0,\mathrm{mod}(2\pi)$.

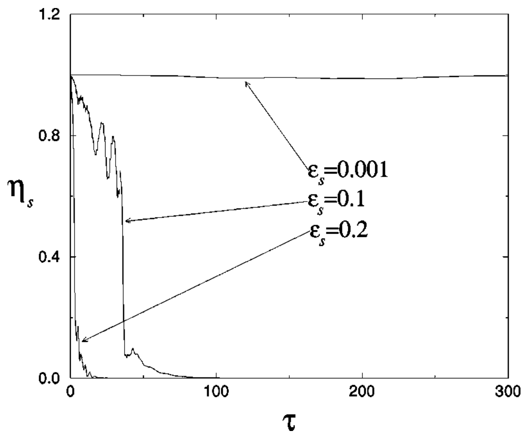

FIG. 5. η_s vs τ for $\eta_0=1.0$, $k=0.5\eta_0^2$, and various values of ε_s.

Solitons can be seen as stable structures if there is a central fixed point surrounded by invariant Kolmogorov-Arnold-Moser [14] curves. The absence of stable equilibria is read as an indication that solitary lumps decay. In this paper, we focus on the most dramatic case of $k<\eta_0^2=W^2\pi/4$. As mentioned, in this regime there is no radiative processes whatsoever when A is small enough. Thus, this is the most neat setting to diagnose breakdown of the quiescent approach. In Fig. 2, we look at phase plots for a series of values of the ratio $\varepsilon\equiv A/\eta_0^2$ with $\eta_0=0.2$, which are listed in the respective captions (ε represents the ratio A/η_0^2 in the surface-of-section plots, ε_s is the corresponding ratio used in the full simulations). At $\varepsilon=2.4$ the soliton has just became unstable prior to chaos. η_s versus time of Fig. 3 seems to agree with the low-dimensional predictions: the peak keeps its integrity up to and probably past $\varepsilon_s\sim1.0$, displaying a slow decaying profile at $\varepsilon=2.0$ and a much faster decay for larger values like $\varepsilon_s=3.0$. The situation becomes even more appealing when larger values of η_0 are considered. To examine the case, we take $\eta_0=1.0$ again for $k=0.5\eta_0^2$. What becomes clear in Fig. 4 is that solitons loose stability for far smaller values of ε, if compared to those of $\eta_0=0.2$; at $\varepsilon\sim0.14$ the soliton is already unstable and the quiescent model, therefore, should no longer be expected as accurate. We then run full simulations for $\eta_0=1.0$ as represented in Fig. 5 and indeed see that the solitonic peak exists only for much smaller values of ε_s than previously. The relevant point we wish to make here is that for larger η_0's, the parametric region $\varepsilon_s\ll1$ which was thought to be safely described by the quiescent approach, is already endangered by nonintegrable features. As a final indication on how much more unstable are larger amplitude solitons, we display the space-time history of the field $|E(x,t)|$ in Fig. 6. The parameters are identical to those used in the case $\varepsilon_s=0.1$ of Fig. 5. Figure 6 shows that the fast decay observed in Fig. 5 really corresponds to soliton destruction and radiation emission. The figure also validates the use of our localized ansatz solution, since prior to decay into radiation $E(x,t)$ resembles a solitary mode. Radiation is damped by dissipation before reaching the borders. To summarize, in the present work, we analyze the validity range of quiescent approximations in the dynamics of solitary waves perturbed by strong external agents; average Lagrangian and simulations are used. We find out that while the validity range of the quiescent approach is large for small soliton amplitudes $\eta_0\ll1$, it becomes noticeably narrower as the amplitude raises up to $\eta_0\lesssim1$. If k is defined in the form $k=\text{const}\,\eta_0^2$ with const $\sim O(1)$ as we did in this paper, the exponential in formula (5) reads $e^{-\text{const}\,\eta_0^2}$. Therefore, when $\eta_0\rightarrow1$, one may expect that various resonances become active (one cannot approximate $e^{-\text{const}\,\eta_0^2}\sim1$ as in the case $\eta_0\ll1$) driving an earlier transition to widespread chaos with destabilization of solitonic fixed points. In qualitative terms, the above reasoning may explain the shortening of the stability range as η_0 raises.

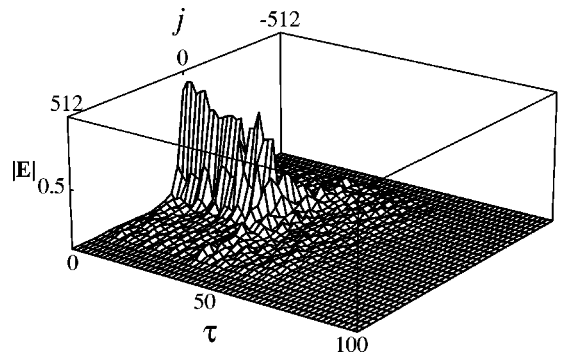

FIG. 6. Space-time history of the quantity $|E(x,t)|$ for the case $\varepsilon_s=0.1$ of Fig. 5. $\eta_0=1.0$.

F.B.R. and A.C.-L.C. wish to express their gratitude to Professor A.W. Thomas and Professor A.G. Williams of the NITP/CSSM—University of Adelaide, Australia, for their hospitality. This work was supported by CNPq and AFOSR.

[1] Y.S. Kivshar and B. Malomed, Rev. Mod. Phys. **61**, 763 (1989).
[2] D. Anderson, Phys. Rev. A **27**, 3135 (1983).
[3] S.G. Thornhill and D. ter Haar, Phys. Rep. **43**, 43 (1978).
[4] A.C.-L. Chian and C.F. Kennel, Astrophys. Space Sci. **97**, 9 (1983).
[5] F.T. Gratton *et al.*, Phys. Rev. E **55**, 3381 (1997).
[6] R. Erichsen *et al.*, Phys. Rev. E **58**, 7812 (1998).
[7] G.I. de Oliveira and F.B. Rizzato, Phys. Rev. E **65**, 016604 (2002).
[8] B. Malomed *et al.*, Phys. Rev. E **55**, 962 (1997).
[9] Y. Nogami and F.M. Toyama, Phys. Rev. E **49**, 4497 (1994).
[10] V.E. Zakharov, Zh. Éksp. Teo. Fiz. **62**, 1745 (1972) [Sov. Phys. JETP **35**, 908 (1972)].
[11] E.A. Kuznetsov *et al.*, Physica D **87**, 201 (1995).
[12] P.A. Robinson, Rev. Mod. Phys. **69**, 507 (1997).
[13] P.A. Robinson *et al.*, Phys. Plasmas **3**, 122 (1996).
[14] A. Lichtenberg and A.J. Lieberman, *Regular and Chaotic Dynamics* (Springer, New York, 1991).